Article

Comparison of trends in the Hadley circulation between CMIP6 and CMIP5

Yan Xia [a,b], Yongyun Hu [b,*], Jiping Liu [c]

[a] College of Global Change and Earth System Science, Beijing Normal University, Beijing 100875, China
[b] Laboratory for Climate and Ocean-Atmosphere Studies, Department of Atmospheric and Oceanic Sciences, School of Physics, Peking University, Beijing 100871, China
[c] Department of Atmospheric and Environmental Sciences, University at Albany, State University of New York, Albany, NY 12222, USA

ARTICLE INFO

ABSTRACT

There have been extensive studies on poleward expansion of the Hadley cells and the associated poleward shift of subtropical dry zones in the past decade. In the present study, we study the trends in the width and strength of the Hadley cells, using currently available simulation results of the Coupled Model Intercomparison Project Phase-6 (CMIP6), and compare the trends with that in CMIP5 simulations. Our results show that the total annual-mean trend in the width of the Hadley cells is $0.13° ± 0.02°$ per decade over 1970–2014 in CMIP6 historical All-forcing simulations. It is almost the same as that in CMIP5. The trend in the strength of the Northern-Hemisphere (NH) cell shows much greater weakening in CMIP6 than in CMIP5, while the strength trend in the Southern-Hemisphere (SH) cell shows slight strengthening. Single-forcing simulations demonstrate that increasing greenhouse gases cause widening and weakening of both the NH and SH Hadley cells, while anthropogenic aerosols and stratospheric ozone changes cause weak strengthening trends in the SH cell. CMIP6 projection simulation results show that both the widening and weakening trends increase with radiative forcing.

© 2020 Science China Press. Published by Elsevier B.V. and Science China Press. All rights reserved.

1. Introduction

The Hadley circulation is one of the most important atmospheric circulation systems, so it must have significant responses to global climate changes and consequently lead to regional climate changes. Observations have showed widening trends of the Hadley circulation since 1979 [1], with magnitude of about 1° per decade. The widening of the Hadley circulation is consistent with some other observational metrics, such as poleward displacements of westerly jets [2], extratropical storm tracks [3], and tropical cyclone tracks [4]. Results of these metrics were summarized in Davis and Rosenlof [5]. The poleward expansion of the Hadley cells has substantial impacts on rainfall patterns [6]. Especially, the poleward shift of subtropical dry zones has a considerable impact on extratropical ecosystems and communities over both land and ocean [7–11].

Previous simulation works have also shown widening trends of the Hadley circulation in responding to different radiative forcings [12–15], although simulated trends are generally much weaker than those in observations [16]. These studies showed that anthropogenic forcings (e.g., increasing greenhouse gases (GHGs) [12–15], ozone depletion [17–19], anthropogenic aerosols and tropospheric ozone [20–23]) all played important roles in causing the observed widening trends. Recent studies suggested that natural variations contribute to the observed widening of the Hadley circulation [24,25]. In particular, it was suggested that the Pacific Decadal Oscillation (PDO) plays the major role in causing the observed widening trends, and that anthropogenic radiative forcings are secondary [25].

While the trends in the width of the Hadley circulation are robust and consistent for both observations and simulations, the trends in the Hadley circulation strength are inconsistent in previous studies. Simulation studies all demonstrated consistent weakening trends of the Hadley circulation under global greenhouse warming [26,27]. However, the changes in the strength of the Hadley circulation are inconsistent among reanalysis datasets [27]. Thus, how anthropogenic forcings and natural variabilities influence on the strength of the Hadley circulation requires further studies.

In previous studies, various metrics are used to characterize the poleward expansion of the tropics. Although these metrics all consistently demonstrate widening of the tropics, they have very different responses to climate changes, and some of these metrics

---

are not closely correlated with the Hadley circulation and may not be good indicators of the poleward shift of the subtropical dry zone [26,28]. Thus, we shall mainly focus on the trends of the Hadley circulation in this paper.

In the present study, we compare the trends in both the width and strength of the Hadley circulation between the Coupled Model Intercomparison Project Phase-6 (CMIP6) and CMIP5. This study is motivated by two reasons. First, CMIP6 models generally have higher horizontal resolutions than CMIP5 models, and how different the trends of the Hadley circulation are in the higher resolution CMIP6 models is of interest. Second, it is known that the climate sensitivity of some CMIP6 models is stronger than that in CMIP5 models [29,30], due to updated parameterizations and other model changes. Whether the stronger climate sensitivity would cause greater trends in the width and strength of the Hadley circulation is also of interest to us. We shall examine how natural variations and anthropogenic forcing impact on both the width and strength of the Hadley circulation in CMIP6 simulations.

2. Data and methods

2.1. Data

In this study, we use simulation results from 29 CMIP6 models that currently have model outputs available online. The CMIP6 experimental design can be found in Eyring et al. [31]. The GHGs concentrations for historical simulations are described in Meinshausen et al. [32]. The experimental design of the projection simulations of future climate change, the so-called shared socioeconomic pathways (SSPs), is described in O'Neill et al. [33]. Table S1 (online) lists the models and experiments.

The simulation results include both historical simulations and SSP projection simulations. For historical simulations, we use the results with all forcings, including both natural and anthropogenic forcings (hereafter denoted by All-forcing), and simulation results with individual forcings, such as natural forcing (denoted by Nat), increasing GHGs (denoted by GHG), changes in stratospheric ozone (denoted by StratO3), and anthropogenic aerosols (denoted by Aer), respectively. SSP projections in CMIP6 are similar to the Representative Concentration Pathways (RCPs) in CMIP5. SSPs climate projections are generated with updated versions of climate models that are driven with SSP scenarios based on updated data and more recent emissions. Detailed differences between SSPs and RCPs are described in O'Neill et al. [33]. Here, simulation results from four scenarios, i.e., SSP1-2.6, SSP2-4.5, SSP3-7.0, and SSP5-8.5, are used.

To compare the trends between CMIP6 and CMIP5 simulations, we use outputs from 25 CMIP6 models and the outputs from their CMIP5 versions (detailed descriptions of the models can be found in the website: https://wcrp-cmip.github.io/CMIP6_CVs/docs/CMIP6_institution_id.html). Table S2 (online) lists the models in CMIP5 and CMIP6, their horizontal resolutions, equilibrium climate sensitivities (ECS), and number of runs. The mean horizontal resolutions are 1.76 × 2.08 and 1.53 × 1.83 in latitude and longitude for CMIP5 and CMIP6, respectively. The ensemble mean ECS is 3.13 and 3.77 K for CMIP5 and CMIP6, respectively.

2.2. Methods

The Hadley circulation is defined with the mean meridional mass streamfunction (MMS), which is computed from the zonal mean meridional wind [v]:

$$\psi(p,\phi) = \frac{2\pi a \cos\phi}{g} \int_0^p [v]\mathrm{d}p.$$

Here, $\psi(p,\phi)$ is the MMS at pressure p and latitude ϕ, a is the Earth radius, and g is the gravitational acceleration. The locations of the poleward edges of the Hadley cells are defined as the first zero crossing of the 500 hPa MMS at the poleward side of the Hadley cells. The strength of the Hadley cells is defined as the maximum absolute value of MMS for both cells. We focus on the results for the metric of MMS, as it is the most widely used metric of width of the Hadley cell in the previous studies [1,12,15]. The Hadley cell extent has been computed with a variety of metrics in the previous literature for CMIP5 simulations to ensure the robustness [24,34]. It is found that different metrics yield qualitatively similar results for the simulations.

Firstly, we calculate the trends in width and strength of the Hadley circulation in each available model. Then, the trends of multi-model ensemble mean are calculated by averaging trends over all the models. Following Hu et al. [15] and Allen et al. [16], the uncertainty of trends is calculated from the multi-model ensembles, as twice the standard error, $2 \times \sigma/\sqrt{n}$, where σ is the standard deviation of the trends and n is the number of trends (models) for both CMIP5 and CMIP6 simulations. The four seasons are December-February (DJF), March-May (MAM), June-August (JJA), and September-November (SON).

3. Results

3.1. Historical simulations

Fig. 1a-c shows trends in the width of the Hadley cells, derived from CMIP6 historical simulations over 1970–2014. For the NH cell (Fig. 1a), the natural forcing does not yield any significant trends in the width, except for a rather weak trend in SON. A similar result was also found in CMIP5 [16]. The anthropogenic aerosol forcing has little influence on the width in all seasons, also similar to that in CMIP5 [12]. By contrast, GHG forcing generates significant widening trends of the NH cell in SON and DJF. Stratospheric ozone changes generate a marginally significant trend in JJA. All-forcing simulations generate significant widening in DJF, MAM, and SON. Especially, the largest widening trend, due to All-forcing, is in SON. For the annual-mean NH cell, GHG is the only forcing that generates significant widening trends, and All-forcing simulations yield a significant widening trend of 0.06° ± 0.02° per decade in CMIP6.

For the SH cell (Fig. 1b), the natural forcing does not cause any significant trends in all seasons. Anthropogenic aerosol forcing yields a significant negative trend in austral winter (JJA). Stratospheric ozone changes produce a significant trend in DJF. GHG forcing causes significant widening trends for all seasons. All-forcing simulation also yields significant widening trends for all seasons. These results indicate that GHG forcing contributes to most of the poleward expansion of the southern cell in all seasons, and stratospheric ozone changes play an important role in causing the poleward expansion in DJF. For the annual-mean SH cell, the widening trends is about 0.07° ± 0.01° per decade.

The total trends summed from both cells are shown in Fig. 1c. Natural and anthropogenic aerosol forcing have no significant contributions in all seasons and the annual mean. Stratospheric ozone has significant positive trends in DJF and JJA. GHG forcing produces significant positive trends in DJF, MAM, and SON. All forcing generates significant widening in all seasons. The annual-mean total widening trend is about 0.13° ± 0.02° per decade.

Using simulations from 25 models from CMIP6 and 27 models from CMIP5 (Table S2 online), we compare the widening trends over 1979–2005 for All-forcing simulations between CMIP5 and CMIP6 (Fig. 1d–f). For the NH cell, the widening trends in CMIP6 are slightly greater than that in CMIP5 in DJF, MAM, and SON,
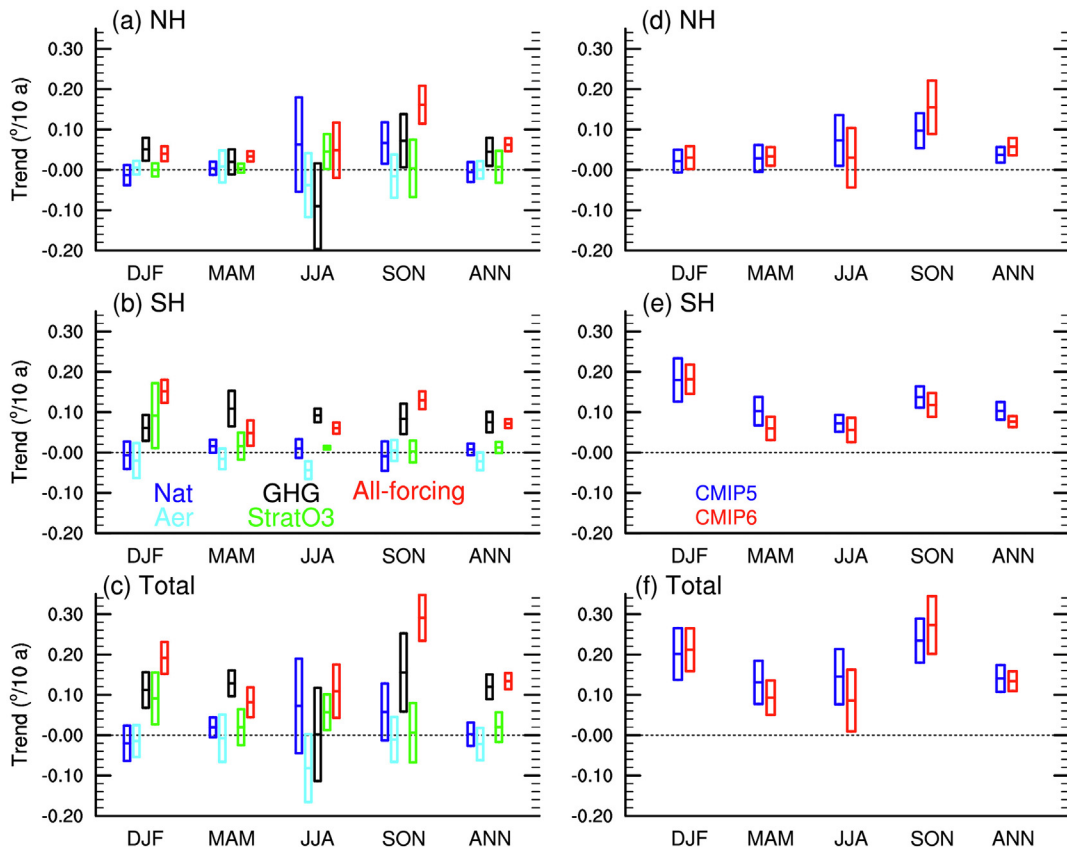
Fig. 1. (Color online) Trends in the width of the Hadley cells, derived from CMIP6 and CMIP5 historical simulations. (a–c) Trends in CMIP6 simulations over the period of 1970–2014; (d–f) comparison of widening trends between CMIP6 and CMIP5 over the period of 1970–2005. (a), (d) NH cell; (b), (e) SH cell; (c), (f) total trends. Positive trends indicate poleward expansion of the Hadley cells and negative values indicate equatorward retreat. Rectangles represent the inter-model 2σ uncertainties (the 95% confidence level). The central lines are the ensemble mean value of trends. Unit is degree in latitude per decade. Hereafter, it is the same for the following figures.

but weaker in JJA. It is worth noting that the widening trends in CMIP5 and CMIP6 simulations show the consistent seasonality, with the largest trend in SON in the All-forcing case. The annual-mean widening trend is about $0.06° \pm 0.02°$ per decade in CMIP6, which is slightly stronger than that in CMIP5 ($0.04° \pm 0.02°$ per decade).

For the SH cell, the largest widening trends in both CMIP6 and CMIP5 are all in DJF, with almost the same values. In other three seasons, the trends in CMIP6 are slightly weaker than that in CMIP5. As a result, the annual-mean widening trend in CMIP6 ($0.08° \pm 0.01°$ per decade) is slightly weaker than that in CMIP5 ($0.10° \pm 0.02°$ per decade). The total widening trends are slightly greater in CMIP6 than in CMIP5 in DJF and SON, but weaker in MAM and JJA. The annual-mean total widening trend is slightly weaker in CMIP6 than in CMIP5 ($0.13° \pm 0.02°$ per decade vs. $0.14° \pm 0.03°$ per decade). Thus, the results here indicate that there is no much difference of the widening trends of the Hadley cells between CMIP6 and CMIP5. As previously published reanalysis-based widening trends cover a large range from ~0.05° per decade to ~1.9° per decade (Table S3 online), the widening trends of the Hadley circulation simulated by both CMIP5 and CMIP6 are within the range of observation.

Fig. 2a, b shows the trends in the strength of the Hadley cells for the period of 1970–2014 for CMIP6 historical simulations. For the NH cell, Nat, Aer, and StratO3 forcings cause insignificant changes of the strength of the Hadley circulation in all seasons. By contrast, GHG forcing causes significant weakening trends in DJF and SON. Results from All-forcing simulations show significant weakening in all seasons, with the largest weakening of $(-0.18 \pm 0.04) \times 10^{10}$ kg s^{-1} per decade in DJF. The net reduction of the NH maximum

MMS is about 0.8×10^{10} kg s^{-1} over 1970–2014. It is about 4% of the climatological mean maximum MMS in DJF. The trend of the annual-mean strength of the NH cell is about $(-0.1 \pm 0.02) \times 10^{10}$ kg s^{-1} per decade, and the annual-mean net reduction is about 5%.

For the SH cell, Nat causes very weak changes in the strength of the maximum MMS. GHG forcing generates significant weakening in MAM and JJA. StratO3 causes strengthening of the SH cell in DJF and MAM. Anthropogenic aerosol forcing causes strengthening trends in JJA and SON. All-forcing simulations generate a significant positive trend in SON. For the annual mean SH cell, All-forcing and StratO3 tend to strengthen the SH cell, while Nat, Aer, and GHG have no significant effects on the annual-mean SH cell. The trends, due to All-forcing and StratO3, are at $(0.05 \pm 0.02) \times 10^{10}$ kg s^{-1} per decade and $(0.03 \pm 0.01) \times 10^{10}$ kg s^{-1} per decade, respectively.

Fig. 2 indicates that GHG forcing results in weakening trends in both NH and SH cells, and that StratO3 and Aer forcings cause weak strengthening of the SH cell. Based on CMIP5 results, Hu et al. [26] pointed out that different radiative forcings have different impacts on the width and strength of the Hadley circulation. They showed that increasing GHGs leads to widening and weakening of the Hadley cells, and that stratospheric ozone depletion (recovery) results in widening (narrowing) of the SH cell, but no effect on the strength of the Hadley cell. Here, the results in CMIP6 are consistent with that in CMIP5. However, anthropogenic aerosol forcing in CMIP6 has a different effect on the strength of the Hadley circulation from that in CMIP5. The CMIP6 results here show that anthropogenic aerosols results in a weak strengthening trend of the SH cell, while such a result was not found in CMIP5 [12].
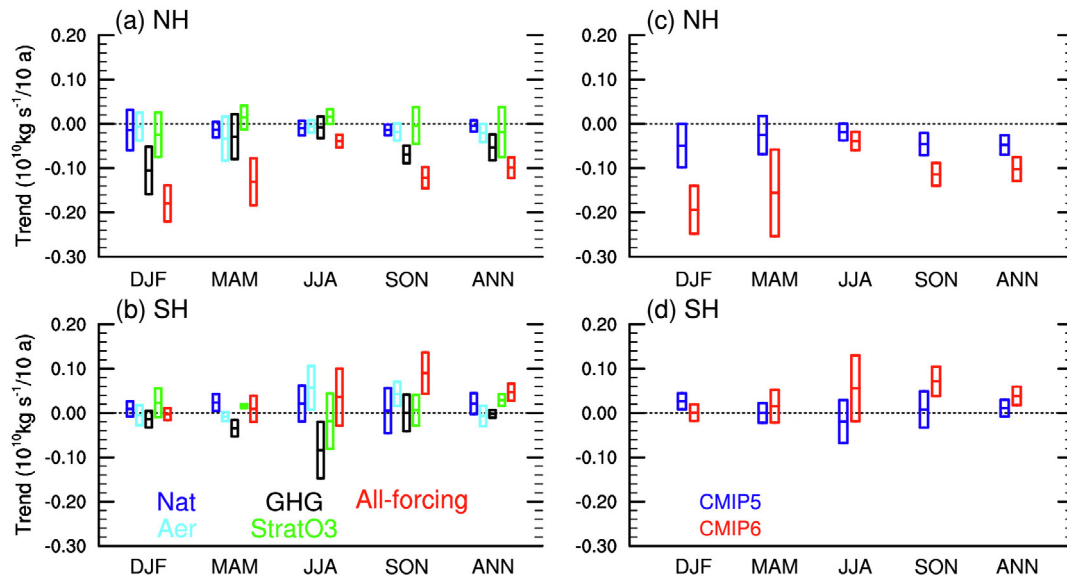
Fig. 2. (Color online) Trends in the strength of the Hadley circulation. (a, b) Trends in CMIP6 simulations over 1970–2014, and (c, d) comparison of strength trends between CMIP6 and CMIP5 over 1970–2005. (a), (c) NH cell; (b), (d) SH cell. Positive/negative trends indicate strengthening/weakening of the Hadley cells. Unit is 10^{10} kg s^{-1} per decade.

Comparison of strength trends of the Hadley cells between CMIP6 and CMIP5 is shown in Fig. 2c, d, using 25 models. The strength trends are calculated from All-forcing simulations over 1979–2005. The weakening trends of the NH cell are much larger in CMIP6 than in CMIP5, especially in DJF and MAM. For the annual mean, the weakening trend in CMIP6 is twice larger than that in CMIP5, i.e., $(0.10 \pm 0.02) \times 10^{10}$ kg s^{-1} per decade vs. $(0.05 \pm 0.02) \times 10^{10}$ kg s^{-1} per decade. However, the SH cell has opposite strength trends to that of the NH cell. Previous studies have also showed significant weakening trends of the NH cell and insignificant trends in the strength of the SH cell in CMIP3 [35] and CMIP5 [36]. In these works, the differences of strength trends between the NH and SH cells were attributed to the inter-hemispheric asymmetry of SST warming patterns. For CMIP6 simulations, the SH shows significant strengthening trends in SON and in the annual mean. Thus, All-forcing has different effects on the strength of the NH and SH cells although they all cause widening trends in both CMIP6 and CMIP5.

Figs. S1 and S2 (online) provide us with an alternative view of trends in the Hadley circulation in CMIP5 and CMIP6, respectively. First, the two figures show high consistencies. The positive trends around 30°N and the negative trends around 30°S in the two figures indicate poleward expansion of the Hadley cells in both hemispheres [12]. The positive trends in the upper tropical troposphere (Figs. S1a, b and S2a, b online) indicate upward expansion of the NH cell. Similarly, the negative trends in the similar region (Figs. S1c, d and S2c, d online) indicate upward expansion of the SH cell. These all reflect deeper ascending motions in the tropical troposphere in All-forcing simulations in both CMIP5 and CMIP6. The upward expansion of the Hadley cell, associated with the upward expansion of the tropopause, is a robust model projection despite the overall weakening of tropical convections [36,37]. The negative trends that overlap the NH cell and the positive trends that overlap the SH cell indicate weakening of the Hadley cells. The negative trends that overlap the SH cell, especially in Fig. S2c, d (online), indicate strengthening of the SH cell.

Second, Figs. S1 and S2 (online) show differences in trends. The most prominent difference is that the NH cell demonstrates greater weakening in CMIP6 than in CMIP5. This can be seen by comparing Fig. S2a, b, d (online) with Fig. S1a, b, d (online). In CMIP6, the SH

cell demonstrates significant strengthening in JJA and SON (Fig. S2c, d online). By contrast, strength changes in the SH cell are insignificant in CMIP5 (Fig. S1c, d online). In addition, the upward expansion of the Hadley circulation is weaker in CMIP6 than in CMIP5 (e.g., Figs. S2a–c and S1a–c online).

The differences of trends in the Hadley circulation can be better seen from the differences of MMS trends between CMIP6 and CMIP5, as shown in Fig. S3 (online). The weakening trends of the NH Hadley cell are greater in CMIP6 than in CMIP5 in all seasons. The SH cell has greater strengthening trends in CMIP6 than in CMIP5 in SON, but weaker strength trends in DJF. It is noticed that the strength changes of the Hadley cells are mainly associated with the ascending branch.

In addition to the changes of the Hadley cells, the Ferrel cells also demonstrate significant changes in both CMIP5 and CMIP6. The NH Ferrel cell shows consistent weakening and northward shift in JJA and SON in both CMIP5 and CMIP6, while the changes in DJF and MAM are not significant and not consistent (Figs. S1 and S2 online). In contrast, the SH Ferrel cell shows strengthening and southward shift in all four seasons. It is well known that the Ferrel cells are driven by extratropical eddies, unlike the Hadley cells that are thermally driven. Thus, the poleward shift and strength changes of both NH and SH Ferrel cells are all associated with poleward retreats of extratropical eddies. The poleward eddy retreat is considered one of the reasons in causing poleward expansion of the Hadley circulation [38]. The strengthening SH Ferrel cell and the weakening NH Ferrel cell are also related to opposite changes of extratropical wave activities between two hemispheres. The trends in the strength of the Ferrel cells indicate increasing extratropical wave activity in SH and weakening wave activity in NH. They also indicate changes in spatial distributions of extratropical wave activities because the strength of the Ferrel cells are proportional to the second order derivatives, rather than the strength of wave activity itself.

To address the difference of trends in the Hadley circulation between CMIP6 and CMIP5, especially the difference in strength trends, we plot sea surface temperature (SST) trends in All-forcing historical simulations and their differences in Fig. 3. The common features of SST trends in CMIP5 and CMIP6 are that significant warming trends are over all oceans (Fig. 3a, b), and that
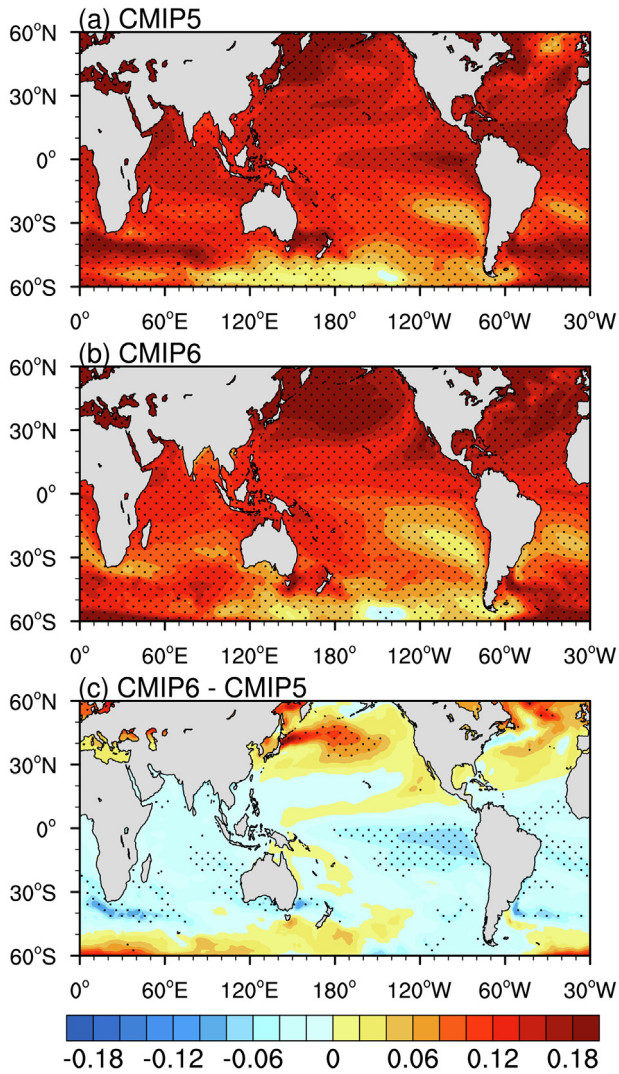
Fig. 3. Ensemble mean and annual mean SST trends in CMIP5 and CMIP6 over 1970–2005. (a) CMIP5; (b) CMIP6; (c) differences of SST trends between CMIP6 and CMIP5. The color interval is 0.02 K/10 a. Dotted areas are the regions that have statistical significance above the 95% confidence level (student's t-test).

suggests that the SH cell would be strengthened. This is consistent with the results in Figs. 2d and S2c, d (online).

Both strength and width trends of the Hadley circulation are also associated with changes in atmospheric thermal structures. Fig. 4a, b shows the trends in zonal and annual mean air temperatures in CMIP5 and CMIP6, respectively. They demonstrate similar trends patterns, with warming in the troposphere and cooling in the stratosphere. However, there are difference of the trends between CMIP6 and CMIP5 (Fig. 4c). CMIP6 shows weaker warming trends in the middle and upper tropics and SH extratropics, but stronger warming trends in the NH extratropics and high latitudes. The differences of atmospheric temperature trends are consistent with the difference of SST trends in Fig. 3c. The trend differences indicate that temperature contrast between the tropics and the NH extratropics are reduced more in CMIP6 than in CMIP5. Thus, extratropical wave activity is weaker in CMIP6, and poleward expansion of the NH cell is slightly greater, as shown in Fig. 1d. In contrast, temperature contrast between the tropics and SH extratropics is slightly greater in the middle and lower troposphere in CMIP6 than that in CMIP5, consistent with the slightly weaker width trend of the SH cell (Fig. 1e).
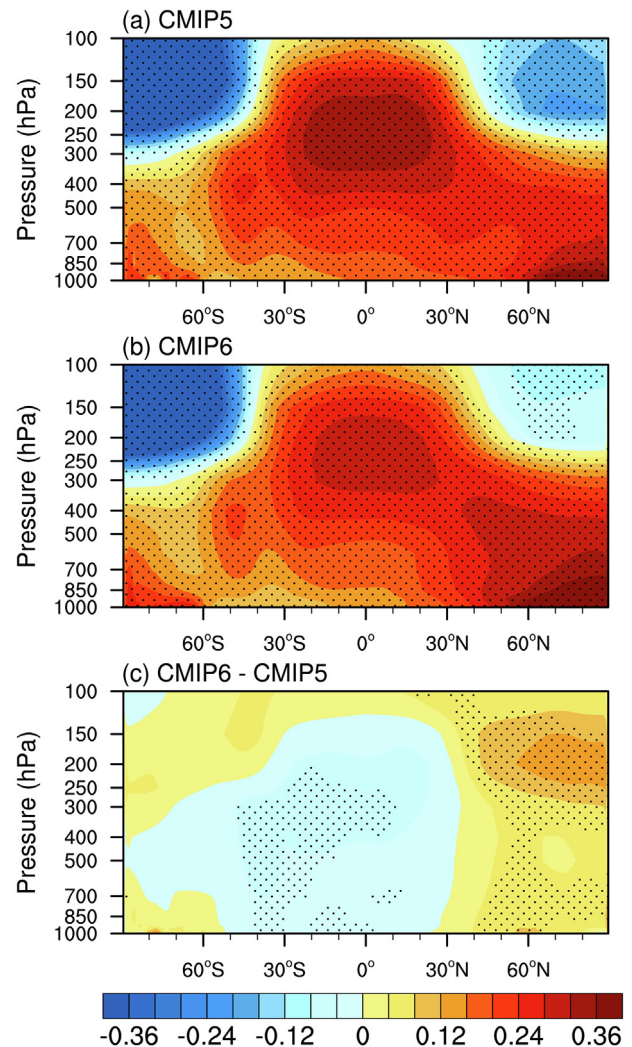
warming trends demonstrate interhemispheric asymmetry, with greater warming trends in NH oceans. The SST trends also demonstrate differences between CMI5 and CMIP6. One of the differences is that CMIP5 shows an "El Niño-like" warming tongue of SST trends, while SST trends in CMIP6 show a "La Niña-like" pattern with relatively weak warming trends along the equator and in the southern and eastern tropical Pacific. The difference of tropical SST trends can be more clearly seen in Fig. 3c. Another difference is that warming trends over Northern Pacific and Atlantic are stronger in CMIP6 than in CMIP5.

Previous studies have argued that spatial patterns of SST trends play the major role in causing strength changes of the Hadley circulation. They showed that uniform SST warming leads to overall weakening of the Hadley circulation, and that the interhemispheric asymmetry of warming trends causes greater weakening of the NH Hadley cell [35,36]. The results here are consistent with their arguments. The differences of tropical SST trends in Fig. 3c suggest that the weakening of the Hadley circulation should be greater in CMIP6 than in CMIP5 because the "El Niño-like" equatorial warming tongue in Fig. 3a would causes less weakening of the Hadley circulation [39]. In addition, the relatively weak warming in the south of the equator of the central and eastern Pacific in Fig. 3b

Fig. 4. Zonal and annual mean temperature trends in CMIP5 and CMIP6 over 1970–2005. (a) CMIP5; (b) CMIP6; (c) differences of temperature trends between CMIP6 and CMIP5. The color interval is 0.06 K/10 a. Dotted areas are the regions that have statistical significance above the 95% confidence level (student's t-test).
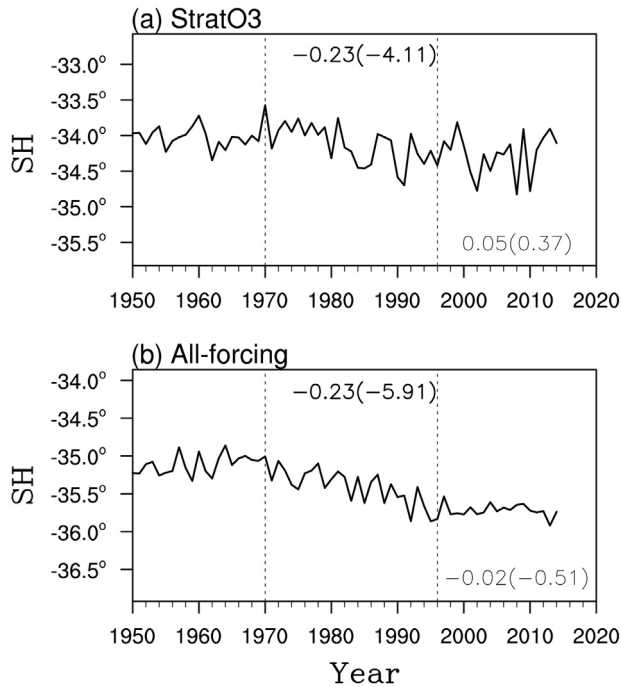
Fig. 5. Time series of multi-model ensemble mean poleward-edge latitudes of the SH cell in DJF in CMIP6. (a) StratO3; (b) All-forcing. The trends are labelled in the plots. The trends are for two time periods: 1970–1996 and 1997–2014. Numbers in the brackets are values of student's *t*-test. Trends over 1970–1996 are statistically significance above the 95% confidence level (labelled in bold), while the trends over 1997–2014 are insignificant.

It is important to point out that the impact of stratospheric ozone changes (depletion/recovery) on the Hadley circulation is different from other forcings. It is known that stratospheric ozone depletion started from the 1970s to the late 1990s, and that stratospheric ozone has shown gradual increasing in the past two decades. Tao et al. [12] have noticed that the SH cell showed equatorward retreat in DJF in CMIP5 since the late 1990s. Here, we show how the SH cell responds to stratospheric ozone changes in CMIP6. Fig. 5a shows the time series of the poleward-edge latitudes of the SH cell in DJF in the case with StratO3 forcing. It can be seen that the SH cell shows poleward expansion over 1970–1996, and that such a tendency stops in the late 1990s. In fact, the trend over 1970–1996 is statistically significant, with a value of −0.23° per decade, while that trend over 1997–2014 is rather weak and positive, about 0.05° per decade, indicating slight equatorward retreat of the SH cell. All-forcing simulations show similar result (Fig. 5b). The time series has a turning point around 1996. The trend over 1970–1996 is also −0.23° per decade. By contrast, the trend over 1997–2014 is only −0.02° per decade. Fig. 5 indicates that the width of the SH cell is sensitive to the changes in the ozone layer. Before the late 1990s, ozone depletion, especially the Antarctic ozone hole, contributes to the widening of the SH Hadley cell. The gradual increasing of Antarctic stratospheric ozone in the past two decades leads to a narrower trend of the SH cell. Thus, the impact of stratospheric ozone on the SH cell will be reversed in the 21st century when the ozone hole will be recovered.

3.2. Projection simulations

In this section, we analyse the trends in CMIP6 projection simulations for the 21st century. Fig. 6a–c shows trends in the width trends over 2016–2100. For the NH cell (Fig. 6a), SSP1-2.6 causes
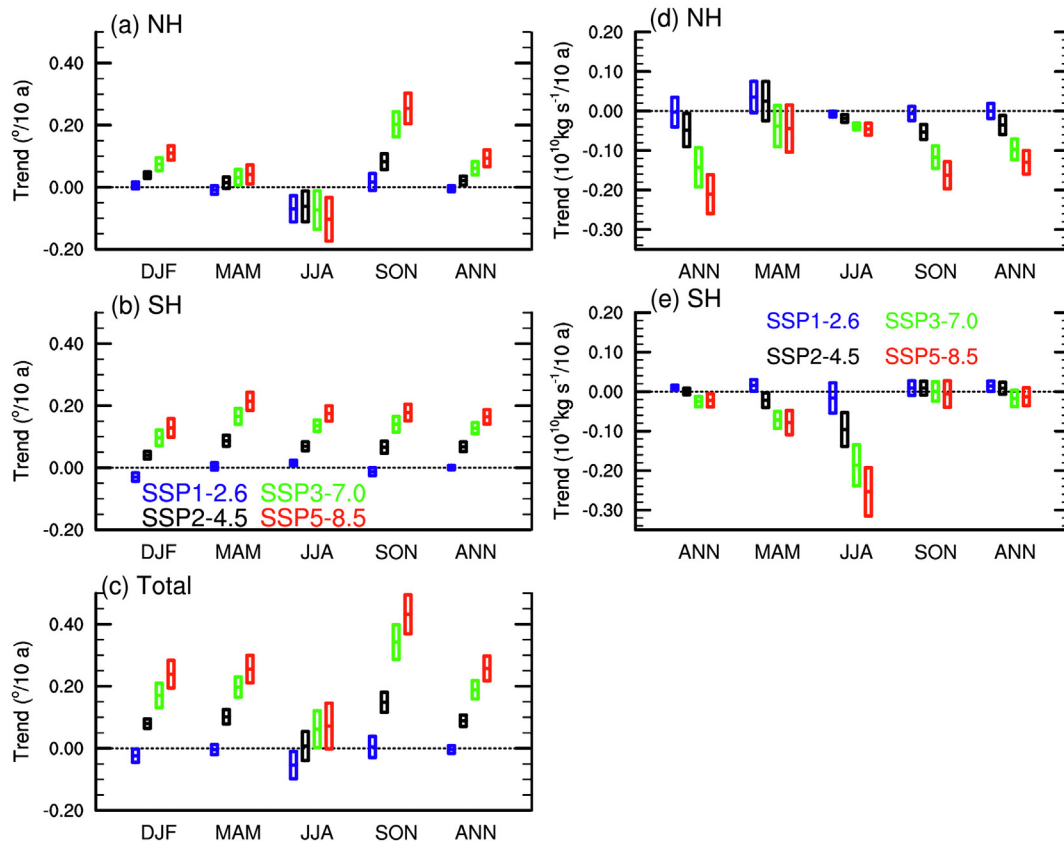

Fig. 6. (Color online) Trends in the width and strength of the Hadley cells for CMIP6 projection simulations over 2016–2100. Left panels: trends in the width for (a) NH cell, (b) SH cell, and (c) total width trends. Unit is degree per decade. Right panels: trends in the strength for (d) NH cell and (e) SH cell. Unit is 10^{10} kg s^{-1} per decade. In (d) and (e), positive (negative) trends indicate strengthening (weakening) of the Hadley circulation.

insignificant changes in the width. For other three projections, the magnitudes of the widening trends increase with radiative forcing in DJF, MAM, and SON. A previous study also showed seasonal variations of width trends in the Hadley circulation in CMIP5 [15]. The negative trends in JJA indicate equatorward retreat of the NH cell. However, it is worth noting that the NH cell is weakest in JJA, and that the noise-signal ratio of MMS is large. Thus, calculations of the poleward boundary of the NH cell and the width trends are not reliable. The largest trends for the four projection scenarios all occurred in SON, consistent with results in CMIP5 RCP projections.

For the SH cell (Fig. 6b), SSP1-2.6 yields weak trends in all seasons. It is important to note that there are significant negative trends in DJF and SON. The negative trends could be a result of the recovery of the Antarctic ozone hole in the 21st century. Because the GHG forcing in the SSP1-2.6 scenario is weak, the effect of ozone recovery on the SH cell can be more important than the GHG forcing and causes the equatorward retreat in DJF and SON. The other three SSPs all generate significant poleward expansion of the SH cell in all seasons, and the trends increases with radiative forcing. The trends in the SH cell have weaker seasonal variations compared with the trends in the NH cell. The total widening trends are shown in Fig. 6c. The largest widening trends are in SON. For SSP3-8.5, the widening trend is $0.42° ± 0.03°$ per decade. Comparison of Fig. 6a-c with Fig. 3 in Hu et al. [15] indicates that the widening trends in CMIP6 have no much differences from that in CMIP5.

Fig. 6d, e shows the trends in the strength of the Hadley circulation over 2016–2100. For the NH cell (Fig. 6d), SSP1-2.6 yields insignificant strength trends in all seasons, while the other three SSPs all generate significant weakening trends DJF, JJA and SON. The magnitudes of the weakening trends increase with radiative forcing. The largest weakening occurs in DJF. For the annual-mean NH cell, the weakening trend caused by SSP5-8.5 is $(0.13 ± 0.03) × 10^{10}$ kg s^{-1} per decade. The net weakening of the annual-mean maximum of the NH is about 10% over the period of 2016–2100.

For the Hadley cell in the SH (Fig. 6e), the trends in strength are relatively weak in DJF and SON. The largest weakening trends are in JJA, in which the weakening trends increase with radiative forcing. The largest weakening trends in JJA are $(0.25 ± 0.06) × 10^{10}$ kg s^{-1} per decade for SSP5-8.5. For the annual-mean SH cell, trends are weak and insignificant for all the four SSP scenarios.

4. Conclusions

We have studied the strength and width trends in the Hadley circulation in CMIP6 simulations. For the NH cell, increasing GHGs plays the major role in causing widening trends of the Hadley circulation, while radiative forcings of stratospheric ozone and anthropogenic aerosols have little impact on the width of the NH cell. All-forcing simulations generate widening trends in DJF, MAM, and SON, and the largest trend is in SON. For the SH cell, increasing GHGs cause significant widening trends in all seasons, and stratospheric ozone changes also leads to widening trends in DJF. Anthropogenic aerosols have little impact on the width of the SH cell.

The trends in CMIP6 are compared with that in CMIP5. In general, the trends in the width of the Hadley cells in CMIP6 have no much difference from that in CMIP5. The width trend of the NH cell is only slightly greater in CMIP6 than in CMIP5 (Fig. 1d), while the width trend of the SH cell is slightly smaller in CMIP6 (Fig. 1e). The total annual-mean widening trend is $0.13° ± 0.02°$ per decade in CMIP6, slightly weaker than that in CMIP5 (Fig. 1f). It appears that the width trends are not sensitive to model resolutions and climate sensitivity.

However, the trends in the strength of the Hadley circulation demonstrate large differences between CMIP6 and CMIP5. The

weakening trends in the NH cell are twice greater in CMIP6 than in CMIP5 for All-forcing simulations, and GHG forcing is the major forcing in causing the weakening trend of the NH cell. For the SH cell in CMIP6, GHG forcing also causes weakening trends, while both stratospheric ozone depletion and anthropogenic aerosols cause strengthening of the SH cell. In CMIP5, the SH cell does not show significant changes. The strengthening trends of the SH cell is generally stronger in CMIP6 than in CMIP5.

The differences of strength trends between CMIP6 and CMIP5 are largely due to different spatial patterns of SST warming trends in the two versions of CMIP models. SST trends show an "El Niño-like" warming pattern in CMIP5. In contrast, SST trends in CMIP6 show a "La Niña-like" warming pattern. In addition, SST warming trends in the NH extratropics are stronger in CMIP6 than those in CMIP5. Such spatial patterns lead to greater weakening of the NH cell and the slightly strengthening of the SH cell in CMIP6.

The All-forcing and StratO3 simulations all show that the width of the SH cell is sensitive to stratospheric ozone changes in DJF. As shown in Fig. 5, the SH cell shows robust widening trend in DJF before 1996. By contrast, the SH cell shows no significant trend in DJF after 1996. This is consistent with results in CMIP5 [12].

Consistent with CMIP5, projection simulations in CMIP6 show that the magnitudes of the widening trends increase with radiative forcing. The largest widening trends in the NH cell demonstrate seasonal variations, and the largest widening trend is in SON. By contrast, the widening trends of the SH cell show much weaker seasonal variations. The Hadley circulation in CMIP6 projection simulations show weakening trends, and the trends increases with radiative forcing. The largest weakening trend occurs in the winter season for both hemispheres.

To compare the trends in CMIP simulations with that in reanalyses, we summarize the trends in the Hadley circulation calculated from ten reanalyses in previous studies in Table S3 (online). All the reanalyses show consistent widening trends in the Hadley circulation. The differences among these reanalyses are that they show large spreads of width trends, ranging from $0.05°$ to $1.9°$ in latitude per decade. It appears that the widening trends are much smaller in the new versions of reanalyses (ERA-Interim, NCEP GSFR, JR55, MERRA2) than those in the old versions (NCEP/NCAR, ERA40, NCEP/DOE, 20CR2, JR25, and MERRA). The width trends in the old version of reanalyses are generally larger than $1.0°$ per decade, while they are about $0.5°$ per decade in the new versions. The width trends in the new versions of reanalyses have smaller differences from simulated trends in CMIP models. In contrast, most reanalyses yield strengthening trends, which are opposite to simulated weakening trends in the Hadley circulation. Why the strength trends are opposite between simulations and reanalyses remains a problem for future studies.

Conflict of interest

The authors declare that they have no conflict of interest.

CMIP6 and ESGF. The CMIP6 model data are available from the ESGF at https://esgf-node.llnl.gov/search/cmip6/.

Author contributions

Yongyun Hu designed the study. Yan Xia analyzed the model outputs and generated figures. Yongyun Hu and Yan Xia wrote the paper with contributions from Jiping Liu.

Appendix A. Supplementary materials

Supplementary materials to this article can be found online at https://doi.org/10.1016/j.scib.2020.06.011.

References

[1] Hu Y, Fu Q. Observed poleward expansion of the Hadley circulation since 1979. Atmos Chem Phys 2007;7:5229–36.
[2] Archer CL, Caldeira K. Historical trends in the jet streams. Geophys Res Lett 2008;35:L08803.
[3] Bender FAM, Ramanathan V, Tselioudis G. Changes in extratropical storm track cloudiness 1983–2008: observational support for a poleward shift. Clim Dyn 2012;38:2037–53.
[4] Studholme J, Gulev S. Concurrent changes to Hadley circulation and the meridional distribution of tropical cyclones. J Clim 2018;31:4367–89.
[5] Davis SM, Rosenlof KH. A multidiagnostic intercomparison of tropical-width time series using reanalyses and satellite observations. J Clim 2012;25:1061–78.
[6] Scheff J, Frierson D. Twenty-first-century multimodel subtropical precipitation declines are mostly midlatitude shifts. J Clim 2012;25:4330–47.
[7] Ye JS. Trend and variability of China's summer precipitation during 1955–2008. Int J Climatol 2014;34:559–66.
[8] Hoerling M, Eischeid J, Perlwitz J, et al. On the increased frequency of Mediterranean drought. J Clim 2012;25:2146–61.
[9] Cayan DR, Das T, Pierce DW, et al. Future dryness in the southwest US and the hydrology of the early 21st century drought. Proc Natl Acad Sci USA 2010;107:21271–6.
[10] Post DA, Bertrand T, Chiew FHS, et al. Decrease in southeastern Australian water availability linked to ongoing Hadley cell expansion. Earths Future 2014;2:231–8.
[11] Feng S, Fu Q. Expansion of global drylands under a warming climate. Atmos Chem Phys 2013;13:10081–94.
[12] Tao LJ, Hu YY, Liu JP. Anthropogenic forcing on the Hadley circulation in CMIP5 simulations. Clim Dyn 2016;46:3337–50.
[13] Grise KM, Polvani LM. Is climate sensitivity related to dynamical sensitivity? J Geophys Res Atmos 2016;121:5159–76.
[14] Lu J, Vecchi GA, Reichler T. Expansion of the Hadley cell under global warming. Geophys Res Lett 2007;34:L06805.
[15] Hu Y, Tao L, Liu J. Poleward expansion of the Hadley circulation in CMIP5 simulations. Adv Atmos Sci 2013;30:790–5.
[16] Allen RJ, Norris JR, Kovilakam M. Influence of anthropogenic aerosols and the pacific decadal oscillation on tropical belt width. Nat Geosci 2014;7:270–4.
[17] Min SK, Son SW. Multimodel attribution of the Southern Hemisphere Hadley cell widening: major role of ozone depletion. J Geophys Res Atmos 2013;118:3007–15.
[18] Son SW, Gerber EP, Perlwitz J, et al. Impact of stratospheric ozone on Southern Hemisphere circulation change: a multimodel assessment. J Geophys Res Atmos 2010;115:1–18.
[19] Waugh DW, Garfinkel CI, Polvani LM. Drivers of the recent tropical expansion in the Southern Hemisphere: changing ssts or ozone depletion? J Clim 2015;28:6581–6.
[20] Allen RJ, Sherwood SC. The impact of natural versus anthropogenic aerosols on atmospheric circulation in the community atmosphere model. Clim Dyn 2011;36:1959–78.
[21] Allen RJ, Sherwood SC, Norris JR, et al. Recent Northern Hemisphere tropical expansion primarily driven by black carbon and tropospheric ozone. Nature 2012;485:350–4.
[22] Shen Z, Ming Y. The influence of aerosol absorption on the extratropical circulation. J Clim 2018;31:5961–75.
[23] Kovilakam M, Mahajan S. Black carbon aerosol-induced Northern Hemisphere tropical expansion. Geophys Res Lett 2015;42:4964–72.
[24] Davis N, Birner T. On the discrepancies in tropical belt expansion between reanalyses and climate models and among tropical belt width metrics. J Clim 2017;30:1211–31.
[25] Allen RJ, Kovilakam M. The role of natural climate variability in recent tropical expansion. J Clim 2017;30:6329–50.
[26] Hu Y, Huang H, Zhou C. Widening and weakening of the Hadley circulation under global warming. Sci Bull 2018;63:640–4.
[27] Mitas CM, Clement A. Recent behavior of the Hadley cell and tropical thermodynamics in climate models and reanalyses. Geophys Res Lett 2006;33:313–24.
[28] Waugh DW, Grise KM, Seviour WJM, et al. Revisiting the relationship among metrics of tropical expansion. J Clim 2018;31:7565–81.
[29] Forster PM, Maycock AC, McKenna CM, et al. Latest climate models confirm need for urgent mitigation. Nat Clim Chang 2020;10:7–10.
[30] Zelinka MD, Myers TA, McCoy DT, et al. Causes of higher climate sensitivity in CMIP6 models. Geophys Res Lett 2020;47:e2019GL085782.
[31] Eyring V, Sandrine B, Meehl GA, et al. Overview of the Coupled Model Intercomparison Project Phase 6 (CMIP6) experimental design and organization. Geosci Model Dev 2016;9:1937–58.
[32] Meinshausen M, Vogel E, Nauels A, et al. Historical greenhouse gas concentrations for climate modelling (CMIP6). Geosci Model Dev 2017;10:2057–116.
[33] O'Neill BC, Tebaldi C, Vuuren D, et al. The scenario model intercomparison project (ScenarioMIP) for CMIP6. Geosci Model Dev 2016;9:3461–82.
[34] Watt-Meyer O, Frierson DMW, Fu Q. Hemispheric asymmetry of tropical expansion under CO_2 forcing. Geophys Res Lett 2019;46:9231–40.
[35] Ma J, Xie SP. Regional patterns of sea surface temperature change: a source of uncertainty in future projections of precipitation and atmospheric circulation. J Clim 2013;26:2482–501.
[36] He J, Soden BJ. Anthropogenic weakening of the tropical circulation: the relative roles of direct CO_2 forcing and sea surface temperature change. J Clim 2015;28:8728–42.
[37] Hartmann DL, Larson K. An important constraint on tropical cloud-climate feedback. Geophys Res Lett 2002;29. 12–1–12–14.
[38] Chen G, Held IM. Phase speed spectra and the recent poleward shift of Southern Hemisphere surface westerlies. Geophys Res Lett 2007;34:L21805.
[39] Lu J, Chen G, Frierson DMW. Response of the zonal mean atmospheric circulation to El Niño versus global warming. J Clim 2008;21:5835–51.

Yan Xia currently works at the College of Global Change and Earth System Science at Beijing Normal University. He finished his B.S. and Ph.D. degrees at Peking University. He is interested in stratospheric climate change and its impact on tropospheric and surface climates and the radiative effects of clouds on global climate change.

Yongyun Hu is a professor at the Department of Atmospheric and Oceanic Sciences, School of Physics at Peking University. He served as the Department Chair and the Vice Dean (2009–2019). He finished his Ph.D. degree at the University of Chicago (1996–2000) and worked as a postdoctoral research associate at University of Washington (2000–2002) and Columbia University (2002–2004). He has broad research interests in present, past, and planetary climates.